Journal of Medicinal Chemistry

Article

Autocorrelation of Molecular Electrostatic Potential Surface Properties Combined with Partial Least Squares Analysis as New Strategy for the Prediction of the Activity of Human A Adenosine Receptor Antagonists

Stefano Moro, Magdalena Bacilieri, Barbara Cacciari, and Giampiero Spalluto

J. Med. Chem., **2005**, 48 (18), 5698-5704• DOI: 10.1021/jm0502440 • Publication Date (Web): 06 August 2005

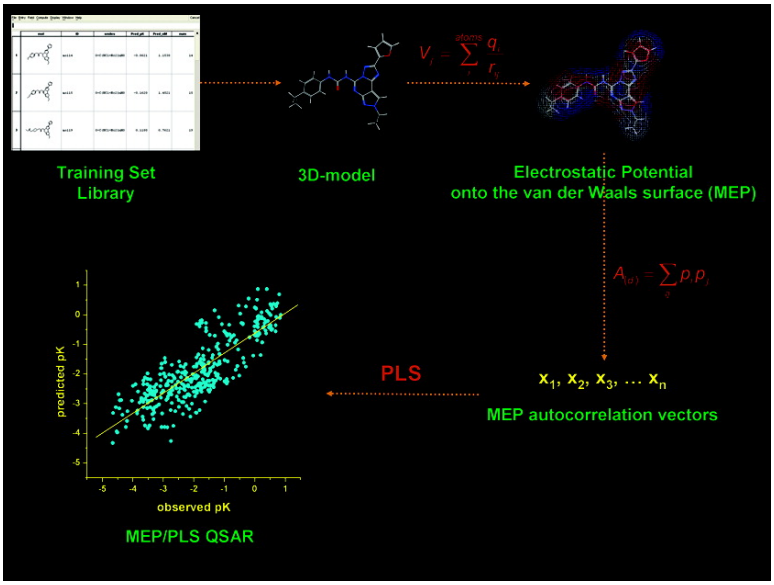

More About This Article

Additional resources and features associated with this article are available within the HTML version:

- Supporting Information
- Links to the 3 articles that cite this article, as of the time of this article download
- Access to high resolution figures
- Links to articles and content related to this article
- Copyright permission to reproduce figures and/or text from this article

View the Full Text HTML

Journal of Medicinal Chemistry is published by the American Chemical Society. 1155 Sixteenth Street N.W., Washington, DC 20036

Autocorrelation of Molecular Electrostatic Potential Surface Properties Combined with Partial Least Squares Analysis as New Strategy for the Prediction of the Activity of Human A_3 Adenosine Receptor Antagonists

Stefano Moro,*,# Magdalena Bacilieri,# Barbara Cacciari,§ and Giampiero Spalluto†

Molecular Modeling Section, Dipartimento di Scienze Farmaceutiche, Università di Padova, via Marzolo 5, I-35131 Padova, Italy, Dipartimento di Scienze Farmaceutiche, Università degli Studi di Trieste, Piazzale Europa 1, I-34127 Trieste, Italy, and Dipartimento di Scienze Farmaceutiche, Università degli Studi di Ferrara, Via Fossato di Mortara 17-19, I-44100 Ferrara, Italy

Received March 16, 2005

The combination of molecular electrostatic potential (MEP) surface properties (autocorrelation vectors) with the conventional partial least squares (PLS) analysis has been used for the prediction of the human A_3 receptor antagonist activities. Three-hundred-fifty-eight structurally diverse human A_3 receptor antagonists have been utilized to generate a novel ligand-based three-dimensional structure−activity relationship. Remarkably, our chemical library includes all 21 important chemical classes of human A_3 antagonists currently discovered, and it represents the largest molecular collection used to generate a general human A_3 antagonist structure−activity relationship. A robust quantitative model has been obtained as described by both cross-validated correlation coefficient ($r_{cv} = 0.81$) and prediction capability ($r_{pred} = 0.82$). The proposed MEP/PLS approach can be considered as an alternative hit identification tool in virtual screening applications.

Introduction

In recent years, we deeply investigated the molecular pharmacology of adenosine receptors and, in particular, the human A_3 adenosine receptor by using an interdisciplinary approach to speed the discovery and structural refinement of new potent and selective A_3 receptor antagonists.[1,2] Briefly, A_3 adenosine receptors (A_3Rs) belong to the adenosine receptor (AR) family of G-protein-coupled receptors (GPCRs), which consists of four distinct subtypes: A_1, A_{2A}, A_{2B}, and A_3. ARs are ubiquitously expressed in the human body.[1,2] The human A_3R (h_A_3R), which is the most recently identified adenosine receptor, is implicated in a variety of important physiopathological processes.[1,2]

Adenosine receptor antagonists, including A_3-selective compounds, have been extensively reviewed in previous articles.[1−4] From a chemical point of view, all known A_3 receptor antagonists can be subdivided into two major groups: (a) purines and structurally related compounds and (b) nonpurine compounds.[4] Considering the "nonpurine derivatives" class, a variety of different heterocyclic nuclei have been identified as potential A_3 adenosine antagonists that can be classified into six major chemical classes: (i) flavonoids, (ii) 1,4-dihydropyridines and pyridines, (iii) triazoloquinazolines, (iv) isoquinoline and quinazolines, (v) pyrazolotriazolopyrimidines, and (vi) several other minor classes. Even if several structure−activity relationships (SARs) have been published on a specific class of human A_3 antagonists,[5−7] a convincing and general quantitative SAR (QSAR) model is still missing. Consequently, the absence of a robust QSAR model drastically limits the application of all ligand-based virtual screening approaches.

Nowadays, the comparative molecular field analysis (CoMFA) methodology is the best known 3D quantitative structure−activity relationship (3D-QSAR) technique that ultimately allows us to design and predict activities of molecules.[8] Typically, a database of molecules with known properties, the training set, is suitably aligned in 3D space according to various methodologies. Superimposition is one of the most crucial steps in CoMFA, and it is based on several techniques including those that maximize the steric overlap, those based on crystallographic data, those based on pharmacophore theory, those employing a steric and electrostatic alignment algorithm, those based on automated field fit methods, and those utilizing pharmacophore mapping programs.[8] Once one has chosen the alignment, charges are calculated for each molecule at an appropriate level of theory. Steric and electrostatic fields are consequently derived for each molecule by the interaction with a probe atom on a series of grid points surrounding the aligned database in 3D space.[8] These field energy terms are then correlated with a property of interest by the use of partial least squares (PLS) with cross-validation, giving a measure of the predictive power of the model. By the very nature of the technique, the most crucial step in this 3D approach is the relative orientation of the test molecules in space.[8] That is, the chosen alignment of the compounds in the training set will have the most profound impact on the predictive ability of the model. We have already noted the plethora of available methods for structural superimposition. We have recently reported that the combination of a target-based

* To whom correspondence should be addressed. Phone: +39 049 827 5704. Fax: +39 049 827 5366. E-mail: stefano.moro@unipd.it.
# Università di Padova.
§ Università degli Studi di Ferrara.
† Università degli Studi di Trieste.

10.1021/jm0502440 CCC: $30.25
Published on Web 08/06/2005

Scheme 1. Structure Classification of All Analyzed Human A_3 Antagonists

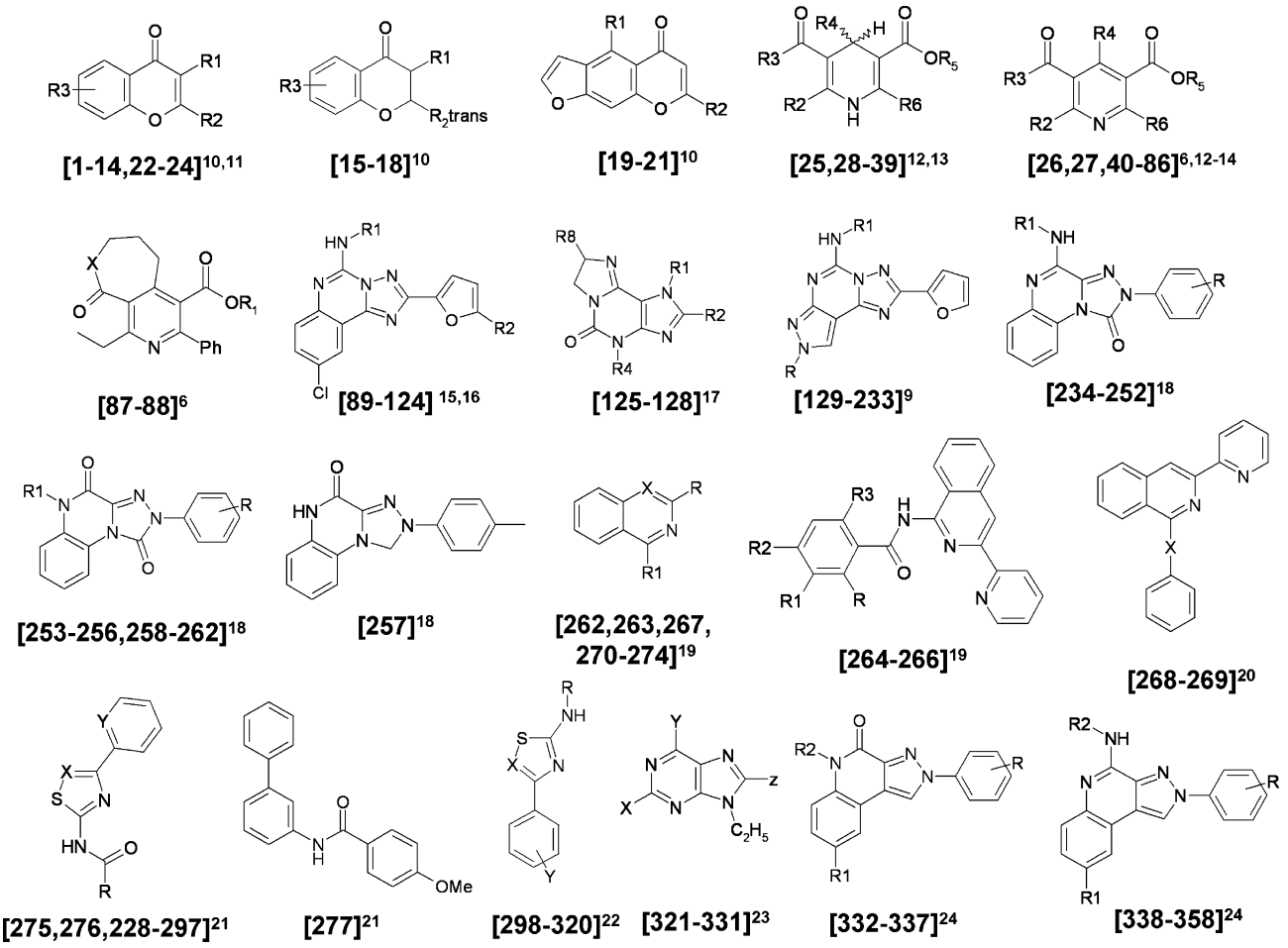

approach, such as high-throughput docking with a quantitative ligand-based methodology such as CoMFA, can improve the capability of discovering new potent and selective human A_3 antagonists.[7] However, the superimposition of chemically diverse classes of compounds, as well as the superimposition of large chemical libraries, can drastically limit the use of CoMFA analysis in all virtual screening applications.

Interestingly, we have recently demonstrated that the application of molecular electrostatic potential (MEP) autocorrelation vectors in tandem with the conventional multivariate PLS analysis approach can be considered a possible alternative strategy to the conventional CoMFA analysis.[9] The peculiarity of this approach is the introduction of autocorrelation vectors as molecular descriptors for the PLS analysis. In particular, the autocorrelation allows the comparison of molecules (and their properties) with different structures and with different spatial orientation without any previous alignment.[9]

In the present paper the combination of molecular electrostatic potential (MEP) surface properties with the conventional partial least squares (PLS) analysis has been used for the prediction of the human A_3 receptor antagonist activities. Three-hundred-fifty-eight structurally diverse human A_3 receptor antagonists have been used to generate a new ligand-based 3D-QSAR. Remarkably, our chemical library includes all 21 important chemical classes of human A_3 antagonists discovered at present, and it currently represents the largest molecular collection used to generate a quantitative model for the human A_3 antagonists (see Scheme 1).

Results and Discussion

Virtual screening of chemical databases is now a well-established method for finding new hit candidates in the drug discovery process. In the present paper, we have developed an integrated approach incorporating the combination of molecular electrostatic potential (MEP) surface properties with the conventional partial least squares (PLS) analysis with the crucial aim of employing a rigorously validated QSAR model for a possible application of virtual screening of available chemical databases for new compounds with high predicted activity.

Gasteiger and collaborators investigated the MEP on a molecular surface as being a particularly useful method for rationalizing the interactions between molecules and molecular recognition processes.[30] Indeed, values and spatial distribution of MEP might strongly influence the binding of a ligand to its active site. Obviously, MEP's property values, as well as other molecular properties, strongly depend on the spatial orientation of the different molecules. Therefore, it is not possible to compare MEP properties of a set of compounds without a previous alignment. As already anticipated, when the compounds in a series are rather similar to one another, it is easy to find a set of hypothetical anchor points and attempt a superimposi-

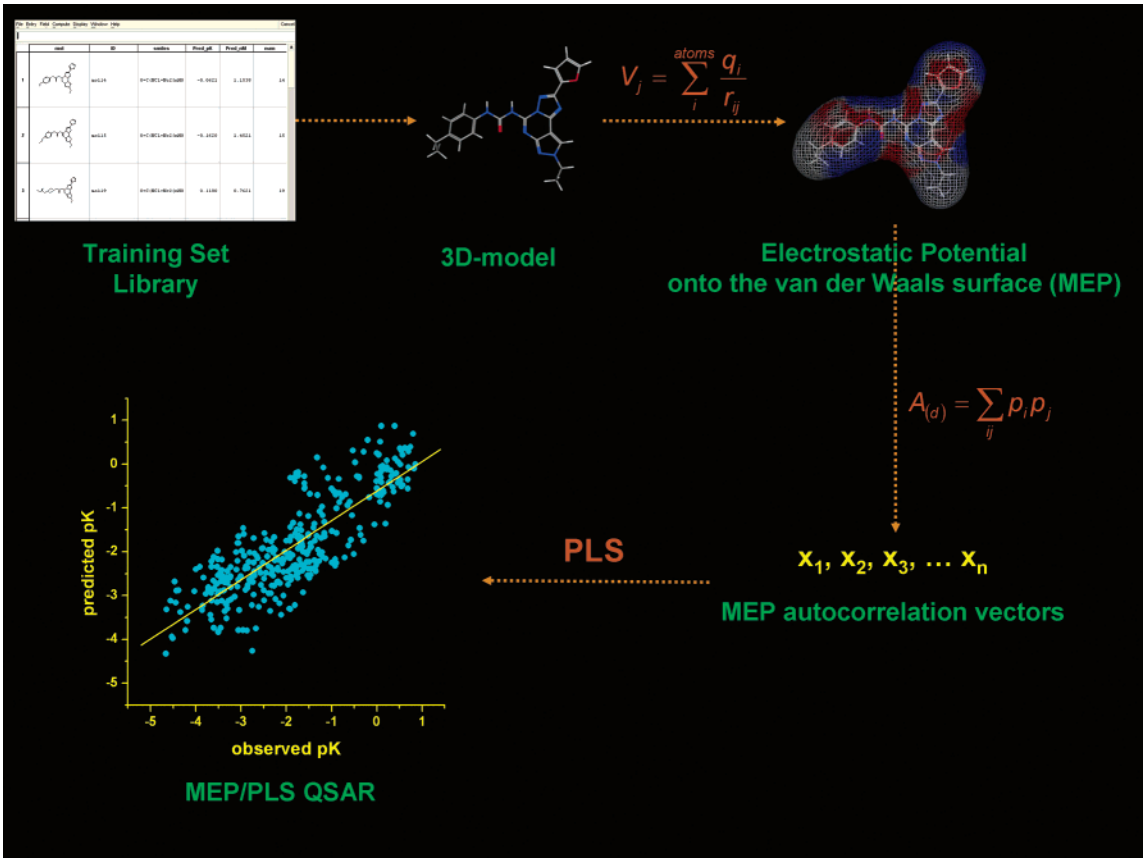

Figure 1. Flowchart describing our combined MEP/PLS QSAR approach.

tion. When the compounds are not so similar, the superimposition is not obvious. The introduction of the autocorrelation vector allows us to overcome this inconvenience, making the MEP information invariant to the spatial rotation and translation of molecules.[30,31] In fact, autocorrelation vector descriptors represent a chemical structure with a vector of fixed length independent of the size of the molecule. Since only internal coordinates (topological or spatial distances of atom pairs or pairs of points on the molecular surface) are taken into account, the resulting descriptors are also independent of the orientation of the molecules in space (translation and rotation invariant). Therefore, no preprocessing alignment of the molecules in a data set is necessary.[30,31] Consequently, we consider this strategy to be very promising for screening very large chemical libraries and to speed the identification of new hit compounds. Even if autocorrelation is potentially useful in medicinal chemistry and, in particular, in developing QSAR models, nowadays only few interesting studies have been reported.[31−37]

The flowchart of our combined MEP and PLS approach is described in Figure 1. As anticipated, 358 structurally diverse human A_3 receptor antagonists, including all 21 important chemical classes of human A_3 antagonists currently discovered, have been utilized to generate our MEP/PLS QSAR. A robust quantitative model has been obtained as described by the cross-validated correlation coefficient (r_{cv} = 0.81, Table 1, Figure 2). To obtain statistical confidence limits, the non-cross-validated analysis was repeated with 10 bootstrap groups, which yielded an r of 0.81 (optimum number of components was 6) and a standard deviation of 0.022. Consistently, a high bootstrapped r value and a small standard deviation suggest a high degree of confidence in the analysis. The bootstrapping method determines the confidence level of a predicted value when a small number of data points are present. An example would be a cross-validation study where the number of points in the training set should be large. This leaves a number of data points in the test set insufficient to generate a confidence level of the accuracy. Instead of using a single set of N data points, the bootstrap method creates a very large number of sets by randomly choosing N members of the set of data points (which obviously means that a single data point may be present more than once in a particular set of

Table 1. Human A_3 MEP/PLS Model: Summary of the Statistic

number of molecules	358
principal components	6
r	0.82
r_{cv} [a]	0.81
r_{bs} [b]	0.81
slope	0.68
offset	−0.61
RMSEC[c]	0.76
$RMSEP_{bs}$ [d]	0.79
SEC[e]	0.77
SEP_{bs} [f]	0.79
bias[g]	5.37 e^{-8}

[a] Cross-validated r^2 after leave-one-out procedure: $r_{cv} = [(SD - PRESS)/SD]^{1/2}$, $SD = (Y_{actual} - Y_{mean})^2$ and $PRESS = \sum(Y_{predicted} - Y_{actual})$. [b] r_{bs} after bootstrapping. [c] Root-mean-square error of calibration: RMSEC. [d] Root-mean-square error of prediction after bootstrapping: $RMSEP_{bs}$. [e] Standard error of calibration: SEC. [f] Standard error of prediction after bootstrapping: SEP_{bs}. [g] Systematic difference between predicted and observed values: bias. For further explanation of these mathematical terms, see ref 45.

Scheme 2. Structure Classification of the Human A_3 Antagonists Used as Test Set

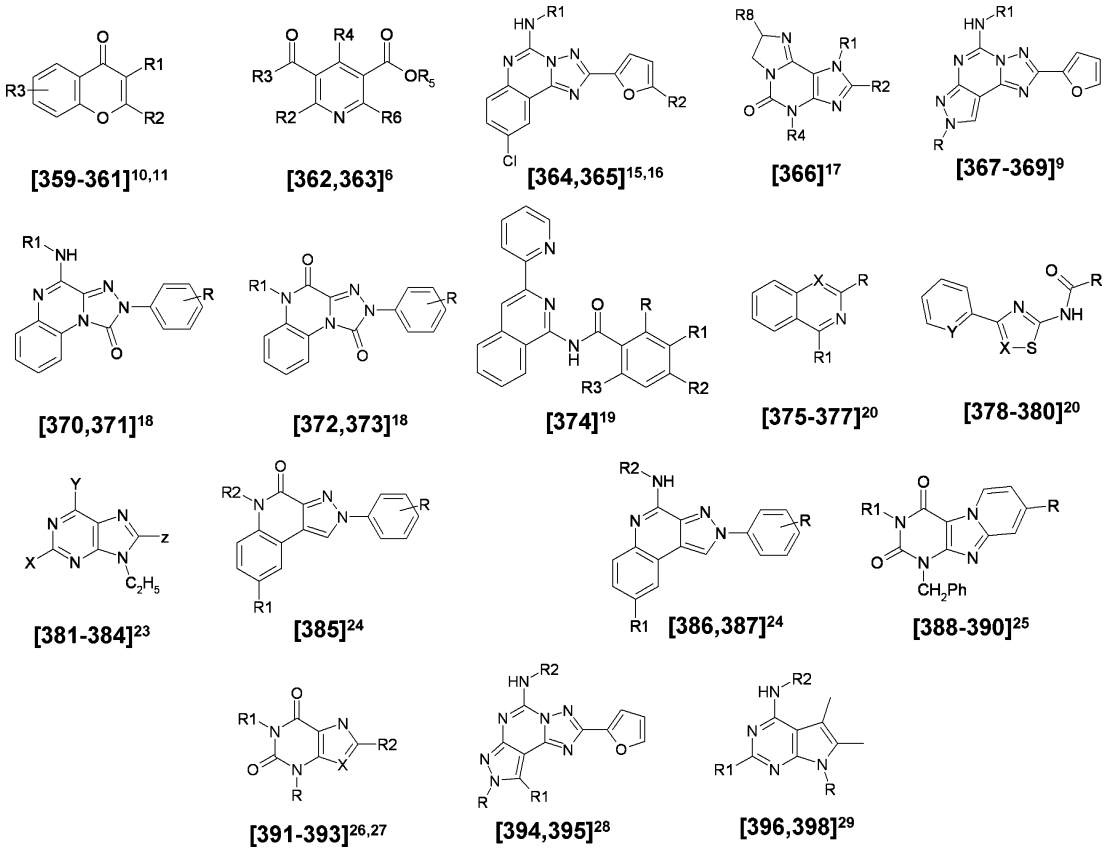

data). This result was unexpected considering both the high level of chemical diversity among the analyzed antagonists and the absence of any molecular alignment procedure (essential and crucial step of the CoMFA methodology).

To validate the obtained MEP/PLS model, we have selected 40 human A_3 receptor antagonists (not included in the original training set) with a different spectrum of structure and affinity (test set, shown in Scheme 2). The selected test set was used to evaluate the predictive power of our MEP/PLS model. As in the calibration step, a similar good predictive ability was obtained (r_{pred} = 0.82) (Table 2). The predicted pK_i were very closed to the experimental values, as shown in Figure 3. Indeed, this is a convincing evidence that the autocorrelated MEP/PLS model is a robust and efficient alternative tool to generate a 3D-QSAR model.

Interestingly our combined MEP/PLS model is able to efficiently discriminate between active and inactive

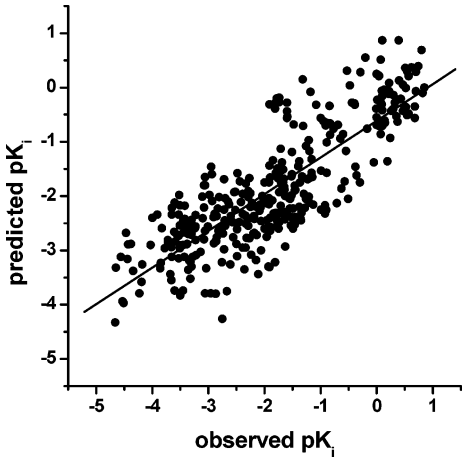

Figure 2. Experimental vs predicted pK_i values obtained by using our combined MEP/PLS QSAR approach.

Table 2. Human A_3 MEP/PLS Model: Validation Protocol

number of compounds	40
r_{pred} [a]	0.82
slope	0.57
offset	−0.92
RMSEP[b]	0.76
SEP[c]	0.75
bias[d]	0.17

[a] The "predictive" r_{pred} was based only on molecules not included in the training set and is defined as explained in ref 34. [b] Root-mean-square error of prediction: RMSEP. [c] Standard error of prediction: SEP. [d] Systematic difference between predicted and observed values: bias.

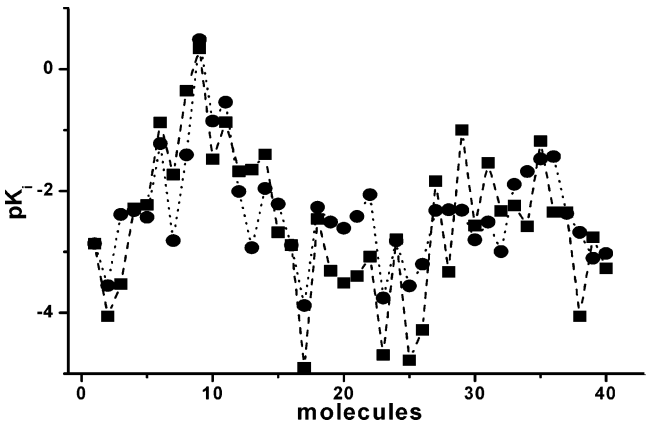

Figure 3. Comparison of experimental pK_i values (■) with those predicted by MEP/PLS QSAR model (●).

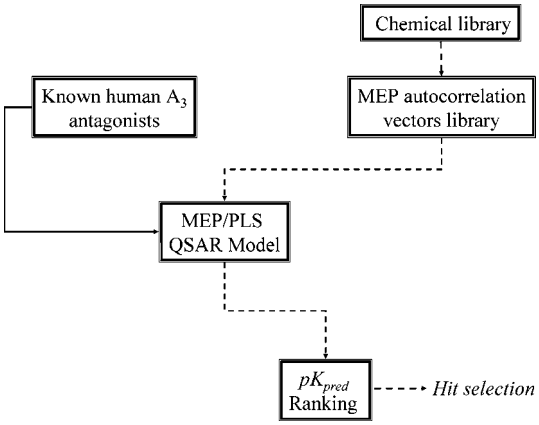

Figure 4. Flowchart describing our combined MEP/PLS QSAR approach in virtual screening applications.

compounds, and this aspect can positively influence its usefulness in virtual screening applications. Considering the peculiarities of our combined MEP/PLS approach, we consider this method to be particularly useful for the hit identification process rather than for lead optimization. In fact, the transformation of MEP surfaces into autocorrelation vectors produces a unique fingerprint of each molecule under consideration. Each fingerprint can be used as input for our combined MEP/PLS model, providing the predicted activity as output. This approach can be considered very useful for a large molecular database screening. Indeed, we are running an intense virtual screening program to validate the real capability of our MEP/PLS model to discover new chemically diverse A_3 antagonists using large (available or virtual) chemical libraries (see Figure 4).

Conclusion

In conclusion, for the first time we have proposed a very general 3D-QSAR model able to rationalize the activity of all known chemical classes of human A_3 adenosine antagonists. We have developed an integrated approach, incorporating the combination of MEP surface properties with conventional PLS analysis to employ a rigorously validated 3D-QSAR model. We are now testing it in possible applications of virtual screening of available chemical databases to discover new compounds with high predicted activity.

Experimental Section

Computational Methodologies. All 3D-QSAR studies were carried out on an eight CPU (PIV 2.0−3.0 GHz) Linux cluster running under openMosix architecture.[38] Autocorrelation MEP studies have been done using the ADRIANA (version 1.0) suite.[39]

Molecular Structure Building. The 3D models of all 358 A_3 antagonists were obtained by using the 3D structure generator Corina. Corina is an integral part of the ADRIANA QSAR suite.[39] Conformer generation and best conformer selection have been carried out using standard parameters of Corina.

Molecular Electrostatic Potential Calculation. In the present work MEPs are derived from a classical point charge model. The electrostatic potential for each molecule is obtained by moving a unit positive point charge across the van der Waals surface, and it is calculated at various points j on this surface by the following equation:[11]

$$V_j = \sum_i^{\text{atoms}} \frac{q_i}{r_{ji}}$$

where q_i represents the partial charge of each atom i and r_{ji} is the distance between points j and atom i. Starting from the 3D model of a molecule and its partial atomic charges, the electrostatic potential or another appropriate property is calculated for points on the molecular surface. Partial atomic charges were calculated by the PEOE method,[40] and its extension to conjugated systems[41] was implemented by the Petra module of the ADRIANA suite.[39] Connolly's solvent accessible surface with a solvent radius of 2.0 Å has been used to project the corresponding MEP. For the pyrazolotriazolopyrimidine derivative **1**, about 3500 points are obtained that are characterized by their Cartesian coordinates and the value of the electrostatic potential. After application of the autocorrelation function, the autocorrelation vector is obtained. Connolly's solvent accessible surface and the corresponding MEP have been calculated by Surface module of ADRIANA.[39]

Autocorrelation Vector. The first application of these vectors as molecular descriptors has been published by Moreau and Broto,[42,43] who applied the classical mathematical notion of an autocorrelation function to the topology of molecular structures. The autocorrelation vector is presented as an intrinsic descriptor of the distribution of an atomic property along the molecular graph. Each component of the autocorrelation vector is calculated as follows:

$$A(d) = \sum_{ij} p_i p_j$$

where A is the autocorrelation coefficient referring to atom pairs ij, p_i is the atomic property, and d is the $i-j$ topological distance.

Starting from this concept, a new 3D descriptor has been introduced that is based on the autocorrelation of properties at distinct points on the molecular surface.[11] The different components of the autocorrelation vector are derived in this way:

$$A(d_{\text{lower}},d_{\text{upper}}) = \frac{1}{L}\sum p_i p_j \qquad (d_{\text{lower}} < d_{ij} < d_{\text{upper}})$$

where the $i-j$ distance d belongs to the d_{lower} and d_{upper} interval and L is number of distances in the same interval. The application of this concept made it possible to compare different molecular properties because this 3D descriptor represents a compressed expression of the distribution of the property p on the molecular surface.[11] The parameters for the calculation of the autocorrelation coefficient are the following: $d_{\text{lower}} = 1$ Å; $d_{\text{upper}} = 13$ Å; $L = 12$; point density is 10 points/Å^2; vdW radius reduction factor is 1.000. All parameters have been changed in various ways to see if it was possible to improve the model capability, but no significant results were derived. Considering distances from 1 to 13 Å with a step width of 1 Å, 12 autocorrelation coefficients are calculated. This transformation produces a unique fingerprint of each molecule under consideration. Autocorrelation vector have been calculated by Surface module of ADRIANA.[39]

Partial Least Squares (PLS) Analysis. All PLS analyses have been carried out using The Unscrambler statistical software.[44]

Test Sets. The test sets consisted of 40 molecules for the considered training set (**359**−**399**; Table 2 of Supporting Information). All predicted activities for the test set molecules were calculated using the autocorrelation MEP/PLS model. The results of the non-cross-validated calibration model on the test sets are summarized in Table 2.

Acknowledgment. We thank Molecular Network GmbH (Erlangen, Germany) for assistance in using the ADRIANA modeling suite. The molecular modeling work coordinated by S.M. has been carried out with

financial support from the Italian Ministry for University and Research (MIUR), Rome, Italy, and from the University of Padova, Padova, Italy. S.M. is also really grateful to Chemical Computing Group for the scientific and technical partnership.

Supporting Information Available: Tables listing binding affinities and p*K* values of training and test sets and a figure of r^2 and q^2 vs number of principal components. This material is available free of charge via the Internet at http://pubs.acs.org.

References

(1) Moro, S.; Deflorian, F.; Spalluto, G.; Pastorin, G.; Cacciari, B.; et al. Demystifying the three dimensional structure of G protein-coupled receptors (GPCRs) with the aid of molecular modeling. *Chem. Commun.* **2003**, *24*, 2949−2956.

(2) Moro, S.; Spalluto, G.; Jacobson, K. A. Techniques: Recent developments in computer-aided engineering of GPCR ligands using the human A_3 adenosine receptor as an example. *Trends Pharmacol. Sci.* **2005**, *26*, 44−51.

(3) Muller, C. E. Medicinal chemistry of adenosine A_3 receptor ligands. *Curr. Top. Med. Chem.* **2003**, *3*, 445−462.

(4) Jacobson, K. A. A_3 adenosine receptors. In *Annual Reports in Medicinal Chemistry*; Doherty, A. M., Ed.; Elsevier: San Diego, CA, 2003; Vol. 38, pp 121−130.

(5) Li, A. H.; Moro, S.; Forsyth, N.; Melman, N.; Ji, X. D.; Jacobson, K. A. Synthesis, CoMFA analysis, and receptor docking of 3,5-diacyl-2,4-dialkylpyridine derivatives as selective A_3 adenosine receptor antagonists. *J. Med. Chem.* **1999**, *42*, 706−721.

(6) Tchilibon, S.; Kim, S. K.; Gao, Z. G.; Harris, B. A.; Blaustein, J. B.; Gross, A. S.; Duong, H. T.; Melman, N.; Jacobson, K. A. Exploring distal regions of the A_3 adenosine receptor binding site: sterically constrained N^6-(2-phenylethyl)adenosine derivatives as potent ligands. *Bioorg. Med. Chem.* **2004**, *12*, 2021−2034.

(7) Moro, S.; Braiuca, P.; Deflorian, F.; Ferrari, C.; Pastorin, G.; Cacciari, B.; Baraldi, P. G.; Varani, K.; Borea, P. A.; Spallato, G. Combined target-based and ligand-based drug design approach as tool to define a novel 3D-pharmacophore model of human A_3 adenosine receptor antagonists: Pyrazolo[4,3-*e*]1,2,4-triazolo[1,5-*c*]pyrimidine derivatives as a key study. *J. Med. Chem.* **2005**, *48*, 152−162.

(8) Kubinyi, H., Folkers, G., Martin, Y. C., Eds. *3D QSAR in Drug Design*; Kluwer: Dordrecht, The Netherlands, 1998; Vols. 2 and 3.

(9) Moro, S.; Bacilieri, M.; Ferrari, C.; Spalluto, G. Autocorrelation of molecular electrostatic potential surface properties combined with partial least squares analysis as alternative attractive tool to generate ligand-based 3D-QSARs. *Curr. Drug Discovery Technol.* **2005**, *2*, 13−21.

(10) Karton, Y.; Jang, J.; Ji, X.; Melman, N.; Olah, M. E.; Stiles, G. L.; Jacobson, K. A. Synthesis and biological activities of flavonoid derivatives as A_3 adenosine receptor antagonists. *J. Med. Chem.* **1996**, *39*, 2293−2301.

(11) Ji, X.; Melman, N.; Jacobson, K. A. Interaction of flavonoids and other phytochemicals with adenosine receptors. *J. Med. Chem.* **1996**, *39*, 781−788.

(12) Van Rhee, A. M.; Jang, J.; Melman, N.; Olah, M. E.; Stiles, G. L.; Jacobson, K. A. Interaction of 1,4-dihydropyridine and pyridine derivatives with adenosine receptors: selectivity for A_3 receptors. *J. Med. Chem.* **1996**, *39*, 2980−2989.

(13) Jiang, J.; van Rhee, A. M.; Melman, N.; Ji, X.; Jacobson, K. A. 6-Phenyl-1,4-dihydropyridine derivatives as potent and selective A_3 adenosine receptor antagonists. *J. Med. Chem.* **1996**, *39*, 4667−4675.

(14) Li, A.; Moro, S.; Melman, N.; Ji, X.; Jacobson, K. A. Structure−activity relationships and molecular modelling of 3,5-diacyl-2,4-dialkylpyridine derivatives as selective A_3 adenosine receptor antagonists. *J. Med. Chem.* **1998**, *41*, 3186−3201.

(15) Kim, Y.; Ji, X.; Jacobson, K. A. Derivatives of triazoloquinazoline adenosine antagonist (CGS15943) are selective for the human A_3 receptor subtype. *J. Med. Chem.* **1996**, *39*, 4142−4148.

(16) Kim, Y.; de Zwart, M.; Chang, L.; Moro, S.; von Frijtag Drabbe Künzel, J. K.; Melman, N.; Ijzerman, A. P.; Jacobson, K. A. Derivatives of the triazoloquinazoline adenosine antagonist (CGS15943) having high potency at human A_{2B} and A_3 receptor subtype. *J. Med. Chem.* **1998**, *41*, 2835−2845.

(17) Müller, C. E.; Thorand, M.; Qurishi, R.; Diekmann, M.; Jacobson, K. A.; Padgett, W. L.; Daly, J. W. Imidazo[2,1-*i*]purin-5-ones and related tricyclic water-soluble purine derivatives: potent A_{2A}- and A_3-adenosine receptor antagonists. *J. Med. Chem.* **2002**, *45*, 3440−3450.

(18) Colotta, V.; Catarzi, D.; Varano, F.; Cecchi, L.; Filacchioni, G.; Martini, C.; Trincavelli, L.; Lucacchini, A. 1,2,4-Triazolo[4,3-*a*]-quinoxalin-1-one: a versatile tool for the synthesis of potent and selective adenosine receptor antagonists. *J. Med. Chem.* **2000**, *43*, 1158−1164.

(19) Van Muijlwijk-Koezen, J. E.; Timmerman, H.; Link, R.; van der Goot, H.; Ijzerman, A. P. A novel class of adenosine A_3 receptor ligands. 2. Structure affinity profile of a series of isoquinoline and quinazoline compounds. *J. Med. Chem.* **1998**, *41*, 3994−4000.

(20) Van Muijlwijk-Koezen, J. E.; Timmerman, H.; van der Goot, H.; Menge, W. M. P. B.; von Drabbe Künzel, J. F.; de Groote, M.; Ijzerman, A. P. Isoquinoline and quinazoline urea analogues as antagonists for the human adenosine A_3 receptor. *J. Med. Chem.* **2000**, *43*, 2227−2238.

(21) Van Muijlwijk-Koezen, J. E.; Timmerman, H.; Vollinga, R. C.; von Drabbe Künzel, J. F.; de Groote, M.; Visser, S.; Ijzerman, A. P. Thiazole and thiazole analogues as novel class of adenosine receptor antagonists. *J. Med. Chem.* **2001**, *44*, 749−762.

(22) Jung, K.; Kim, S.; Gao, Z.; Gross, A. S.; Melman, N.; Jacobson, K. A.; Kim, Y. Structure−activity relationships of thiazole and thiadiazole derivatives as potent and selective human adenosine A_3 receptor antagonists. *Bioorg. Med. Chem.* **2004**, *12*, 613−623.

(23) Camaioni, E.; Costanzi, S.; Vittori, S.; Volpini, R.; Klotz, K.; Cristalli, G. New substituted 9-alkylpurines as adenosine receptor ligands. *Bioorg. Med. Chem.* **1998**, *6*, 523−533.

(24) Colotta, V.; Catarzi, D.; Varano, F.; Cecchi, L.; Filacchioni, G.; Martini, C.; Trincavelli, L.; Lucacchini, A. Synthesis and structure−activity relationships of new set of 2-arylpyrazolo[3,4-*c*]-quinoline derivatives as adenosine receptor antagonists. *J. Med. Chem.* **2000**, *43*, 3118−3124.

(25) Priego, E.; von Frijtag Drabbe Künzel, J.; Ijzerman, A. P.; Camarasa, M.; Pérez-Pérez, M. Pyrido[2,1-*f*]purine-2,4-dione derivatives as novel class of highly potent human A_3 adenosine receptor antagonists. *J. Med. Chem.* **2002**, *45*, 3337−3344.

(26) Hayallah, A. M.; Sandoval-Ramirez, J.; Reith, U.; Schobert, U.; Preiss, B.; Schumacher, B.; Daly, J. W.; Müller, C. E. 1,8-Disubstituted xanthine derivatives: synthesis of potent A_{2B}-selective adenosine receptor antagonists. *J. Med. Chem.* **2002**, *45*, 1500−1510.

(27) Linden, J.; Thai, T.; Fingler, H.; Jin, X.; Robeva, A. Characterization of human A_{2B} adenosine receptors: radioligand binding, Western blotting, and coupling to G_q in human embryonic kidney 293 cells and HMC-1 mast cells. *Mol. Pharmacol.* **1999**, *56*, 705−713.

(28) Baraldi, P. G.; Fruttarolo, F.; Tabrizi, M. A.; Preti, D.; Romagnoli, R.; El-Kashef, H.; Moorman, A.; Varani, K.; Gessi, S.; Merighi, S.; Borea, P. A. Deign, synthesis and biological evaluation of C^9- and C^2-substituted pyrazolo[4,3-*e*]-1,2,4-triazolo[1,5-*c*]pyrimidines as new A_{2B} and A_3 adenosine receptors antagonists. *J. Med. Chem.* **2003**, *46*, 1229−1241.

(29) Hess, S.; Müller, C. E.; Frobenius, W.; Reith, U.; Klotz, K.; Eger, K. 7-Deazaadenines bearing polar substituents: structure−activity relationships of new $A_1$and A_3 adenosine receptor antagonists. *J. Med. Chem.* **2000**, *43*, 4636−4646.

(30) Gasteiger, J.; Li, X.; Rudolph, C.; Sadowsky, J.; Zupan, J. Representation of molecular electrostatic potentials by topological feature maps. *J. Am. Chem. Soc.* **1994**, *116*, 4608−4620.

(31) Wagener, M.; Sadowsky, J.; Gasteiger. J. Autocorrelation of molecular surface properties for modeling corticosteroid binding globulin and cytosolic Ah receptor activity by neural networks, J. *J. Am. Chem.* Soc. **1995**, *117*, 7769−7775.

(32) Clementi, S.; Cruciani, G.; Riganelli, D.; Valigi, R.; Costantino, G.; Baroni, M.; Wold, S. Autocorrelation as a Tool for a congruent description of molecules in 3D QSAR studies. *Pharm. Pharmacol. Lett.* **1993**, *3*, 5−8.

(33) Blin, N.; Federici, C.; Koscielniak, T.; Strosberg, A. D. Predictive quantitative structure−activity relationships (QSAR) analysis of beta 3-adrenergic ligands. *Drug Des. Discovery* **1995**, *12*, 297−311.

(34) Gancia, E.; Bravi, G.; Mascagni, P.; Zaliani, A. Global 3D-QSAR methods: MS-WHIM and autocorrelation. *J. Comput.-Aided Mol. Des.* **2000**, *14*, 293−306.

(35) Pastor, M.; Cruciani, G.; McLay, I.; Pickett, S.; Clementi, S. Grid independent descriptors (GRIND). A novel class of alignment-independent three-dimensional molecular descriptors. *J. Med. Chem.* **2000**, *43*, 3233−3243.

(36) Klein, C. T.; Kaiser, D.; Ecker, G. Topological distance based 3D descriptors for use in QSAR and diversity analysis. *J. Chem. Inf. Comput. Sci.* **2004**, *44*, 200−209.

(37) Gupta, M. K.; Sagar, R.; Shaw, A. K.; Prabhakar, Y. S. CP-MLR directed QSAR studies on the antimycobacterial activity of functionalized alkenols-topological descriptors in modeling the activity. *Bioorg. Med. Chem.* **2005**, *13*, 343−351.

(38) *OpenMosix*; http://www.openMosix.org, 2004.

(39) *ADRIANA*.; Molecular Networks GmbH: Erlangen, Germany, 2003.

(40) Gasteiger, J.; Marsili, M. Iterative Partial equalization of orbital electronegativity. A rapid access to atomic charges. *Tetrahedron* **1980**, *36*, 3219−3228.
(41) Gasteiger, J.; Saller, H. Berechnung der ladungsverteilung in konjugierten systemen durch eine quantifizierung des mesomeriekonzeptes. *Angew. Chem.* **1985**, *97*, 699−701.
(42) Moreau, G.; Broto, P. The autocorrelation of a topological structure: a new molecular descriptor. *Nouv. J. Chim.* **1980**, *4*, 359−360.
(43) Moreau, G.; Broto, P. Autocorrelation of molecular structures. Application to SAR Studies. *Nouv. J. Chim.* **1980**, *4*, 757−764.
(44) *The Unscrambler*, version 9.0; CAMO Process AS: Oslo, Norway 2003.
(45) *Handbook of Computational Statistics: Concepts and Methods*; Gentle, James, E., Härdle, W., Mori, Y., Eds.; Springer-Verlag: New York, 2004.

JM0502440